

## Electrospun Poly(acrylic acid)/Lysine Fibers and the Interactive Effects of Moisture, Heat, and Cross-Link Density on Their Behavior

Niall Finn,<sup>1</sup> Clemence Carlinet,<sup>1,2</sup> George Maurdev<sup>1</sup>

<sup>1</sup>CSIRO Materials Science and Engineering, Waurn Ponds, 3216 Victoria, Australia

<sup>2</sup>Ecole Nationale Supérieure de Chimie, de Biologie et de Physique Bordeaux, 33607 Pessac, France

Correspondence to: N. Finn (E-mail: niall.finn@csiro.au)

**ABSTRACT:** Poly(acrylic acid) (PAA) is an important polymer frequently used as a superabsorbent in health and hygiene products. As a polyelectrolyte that swells with absorption of water it has potential application in other fields including drug delivery, tissue scaffolds, actuators, and desiccation and humidity control. To be useful in such applications the membrane's mechanical integrity must be maintained while optimizing its moisture absorption properties. In this work PAA membranes are electrospun with lysine as cross-linking agent. The effects of varying the concentration of the lysine on the cross-link density and consequently on the thermo- and hygro-mechanical properties of the membranes are studied through electron microscopy, FTIR spectroscopy, and dynamic mechanical thermal analysis (DMTA). Isothermal glass transitions are shown to occur with varying moisture content. The moisture content (or relative humidity) at which the transition occurs is reduced by increasing temperature and can be controlled by varying the cross-link density. © 2014 Wiley Periodicals, Inc. *J. Appl. Polym. Sci.* **2015**, *132*, 41252.

**KEYWORDS:** adsorption; electrospinning; fibers; glass transition; hydrophilic polymers

Received 13 April 2014; accepted 29 June 2014

DOI: 10.1002/app.41252

### INTRODUCTION

Electrospinning is a simple and economical method for producing fibers of small diameter and high surface area. This technique, described in detail elsewhere,<sup>1–4</sup> consists of driving a concentrated polymer solution through an electrified needle, forming a jet of liquid which is then propelled electrostatically onto a conducting surface connected to electrical earth. The solvent evaporates from the jet of liquid producing a nonwoven mat composed of fibers with diameters that may be between a few tens of nanometers and a few microns.<sup>1–4</sup> There are variations on this configuration; however, this is the most common.

The sub-micron and nanoscale fibers most typically produced by electrospinning have a high surface area compared with traditional synthetic fibers, and may be used in filtration<sup>2,5</sup> or ion absorption.<sup>6,7</sup> When water is the electrospinning solvent, water vapor is the only by-product of the process, and any solutes remain in the fiber, resulting in a low environmental discharge. A disadvantage of using water as a solvent is the fibers produced may be dissolved or damaged by high humidity and condensation. To counter this, fibers can be stabilized via chemical crosslinking<sup>8</sup> and photo-crosslinking,<sup>9</sup> rendering the water soluble polymers impervious to water after electrospinning. The thermo-mechanical properties of membranes electrospun from hygroscopic polymers is of interest both to determine the limits

of the range of possible applications and to potentially engineer their properties for specific environmental conditions.<sup>10</sup>

The work presented here consists of the production and stabilization of poly(acrylic acid) electrospun fibers using L-lysine as a crosslinker. The amino acid L-lysine was selected because it is nontoxic and contains two amine groups which can react with carboxylic acids on poly(acrylic acid) via a condensation reaction to produce chemically stable amide linkages. If the two amines in a lysine molecule react with acid groups on adjacent poly(acrylic acid) molecules, covalent crosslinks will be formed. This condensation reaction can be driven forward both kinetically and thermodynamically by heating above 100°C, where the reaction product is driven off as water vapor. The structure and mechanical properties of these fibers are studied, and the improvements in these properties through crosslinking are demonstrated. In contrast to commonly used cross-linkers such as glycerol, lysine, and any amides formed have infrared spectroscopic features distinct from those of PAA and so the degree of crosslinking can be studied using FTIR. The thermo-mechanical properties of the membranes were measured as a function of cross-link density and relative humidity using dynamic mechanical analysis (DMA) with a controlled humidity chamber; varying RH from 10 to 80% and temperatures from 30°C to 80°C. Isothermal glass transitions were observed with varying RH leading to the introduction of the

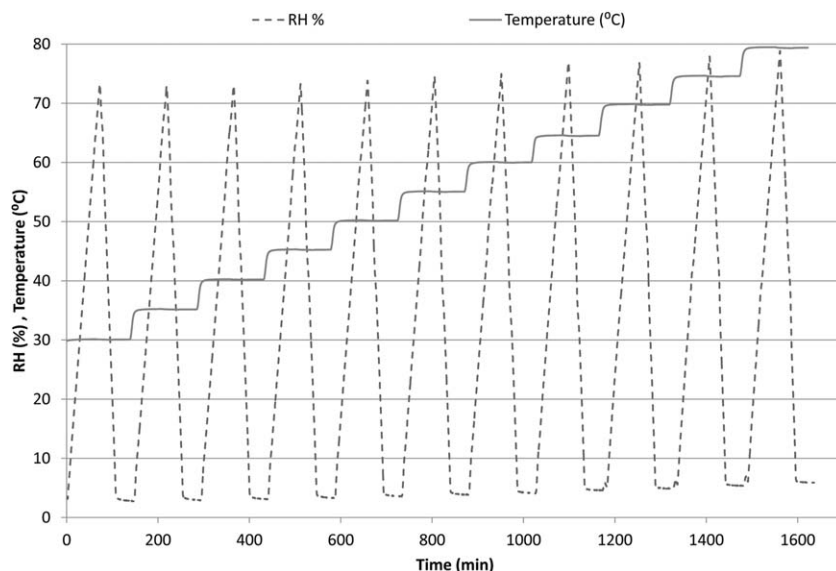


**Figure 1.** Temperature and RH profiles for the DMA experiments.

useful concept of a “glass transition moisture content”  $MC_g$  for hygroscopic polymers, which depends on temperature and cross-link density.

## EXPERIMENTAL

### Materials

Poly(acrylic acid) of molecular weight 400,000 and L-lysine were purchased from Sigma-Aldrich and used as received. All water used was Ultrapure Milli-Q filtered water prefiltered through a R.O. membrane.

### Electrospinning

Electrospun membranes were prepared from aqueous 8.0%w/w poly(acrylic acid). The amino acid L-lysine was incorporated in concentrations of 0 (control), 0.4, 0.8, and 1.6%w/w, which produces a molar ratio of 0, 2.5, 5, and 10% of L-lysine mol/mol relative to carboxylic acid side groups on the polymer. If all the lysine present in each sample forms cross-links then the proportion of cross-linking is 0, 5, 10, and 20% of the maximum available. The electrospinning apparatus comprised a 3-mL syringe, with a stainless steel needle (23G, I.D. 0.6 mm and 24 mm in length). The needle was attached to a high voltage, direct current power supply with a voltage range between 0 and 30 kV; however, the voltage used in this work was 13 kV. The electrospun layer was collected on aluminum foil mounted on a barrel 10 cm in diameter, rotating at 2 m/min. The needle-collector separation was 20 cm and solution injection rate was  $\sim 0.5 \text{ mL h}^{-1}$ .

### Crosslinking

Electrospun nonwoven poly(acrylic acid) layers were crosslinked through the inclusion of L-lysine, and were heated to 140°C, in ambient humidity, for periods between 0 and 2 h.

### Fourier Transform Infrared Spectrometry

Infrared spectra were obtained using a Perkin Elmer Spectrum 100 FTIR Spectrometer, and data logged and processed using the Spectrum 6.3.4 software provided. The ATR accessory was

fitted with a single bounce total internal reflectance “Diamond” crystal, with an angle of incidence of 45°. Samples were in contact with the surface of the crystal, and 64 scans were taken for each measurement.

### Scanning Electron Microscopy

For electron imaging the samples were mounted on stubs using double sided conductive carbon tape and then coated with  $\sim 1 \text{ nm}$  of Pt/Pd using a Cressington 208HR coater to enhance surface conductivity. The samples were then imaged in a Hitachi S4300SE/N field emission scanning electron microscope at high vacuum, a nominal working distance of 10 mm and an electron beam accelerating voltage of 1.2 kV.

### Dynamic Mechanical Analyzer with Controlled Humidity

DMA measurements were performed using a TA systems DMA Q800, with the humidity control attachment. Analysis was performed<sup>11</sup> by mounting a sample  $\sim 6 \text{ mm}$  wide and 20 mm long in the tensile film clamps with a gauge-length of around 10 mm. The sample was then preloaded to 0.1N and tensile oscillation applied with 10  $\mu\text{m}$  amplitude at a frequency of 1 Hz, the force track function was used at 120% to maintain tension in the sample under all conditions. The applied load required to maintain the 10  $\mu\text{m}$  amplitude was measured while varying the humidity from 10 to 75% over  $\sim 100 \text{ min}$  at constant temperature. The humidity was returned to 10% and held for 55 min then the temperature was increased by 5°C and held for another 20 min. The isothermal humidity cycle was repeated at each of 11 temperatures increasing from 30°C to 80°C in 5°C steps, as shown in Figure 1. The dimensions of the samples were variable, sensitive to humidity, and changed during the experiments and so meaningful comparison of the absolute stiffness values was difficult. Therefore, the relative stiffness was calculated for each sample, this being the stiffness at a given RH and temperature expressed as a percentage of the highest stiffness recorded during the scan for that sample. Glass transitions were observed with a rapid drop in stiffness as the relative

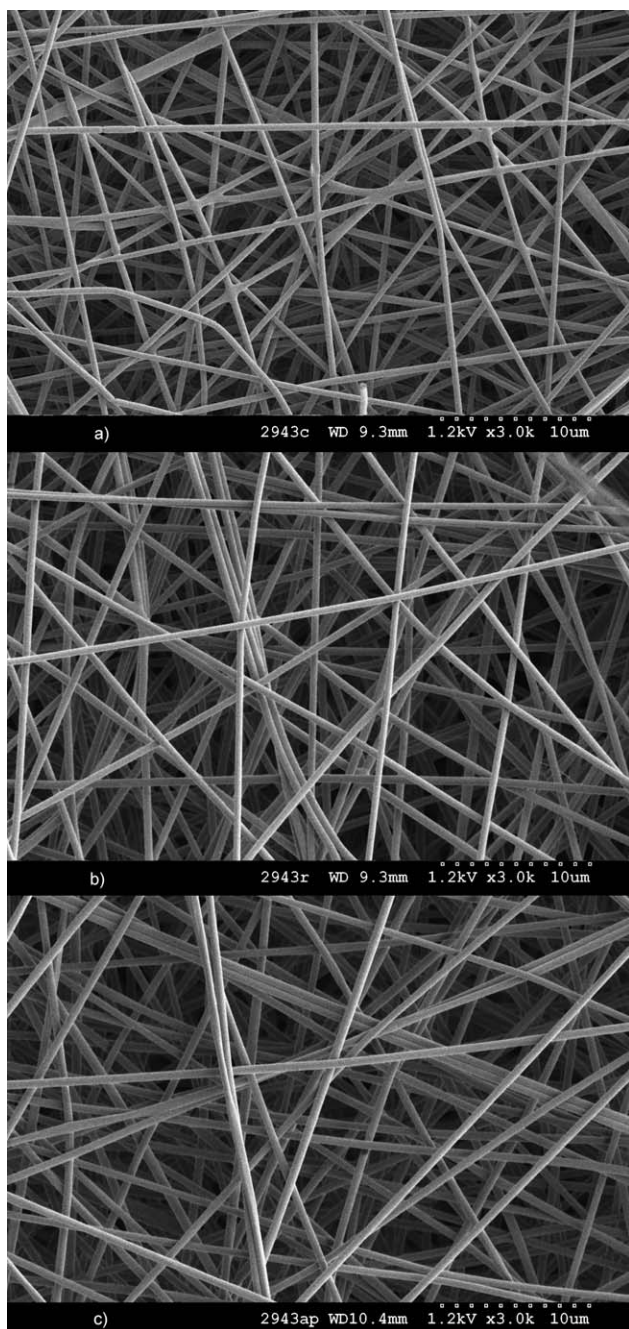


**Figure 2.** Electrospun poly(acrylic acid) membrane, spun from solutions containing 8% poly(acrylic acid), and (a) 0, (b) 0.4, and (c) 1.6% L-lysine mol/mol.

humidity and hence moisture content increased. The glass transition value was defined using the usual “onset” method as being the intersection of the slopes just before and just after the transition in the stiffness-RH or stiffness-moisture content curves.

## RESULTS AND DISCUSSION

Non-woven mats were produced by electrospinning as was described in the experimental section. Poly(acrylic acid) has good solubility and a high density of carboxylic acid groups.

The solutions electrospun well over a range of needle voltages and needle/collector separation distances. Although L-lysine contains a carboxylic acid moiety, the concentration of carboxylic acid groups in the mixture is 90% or more from the polymer, and so the reactions between the amine and carboxylic acid groups would be predominantly between the L-lysine and the polymer.

The membranes had a uniform appearance, and were white as is typically found in electrospun webs. Scanning electron micrographs of the electrospun poly(acrylic acid) mats are shown in Figure 2. The electron micrographs show randomly oriented fibers of regular geometry, and look very typical of images published elsewhere.<sup>1–3</sup> As lysine was included there was very little variation in the formation of fibers, with each image showing very little interconnection of fibers, which would be caused by the fibers not being completely dry upon collection. Optimization of the liquid flow rate and the electrode spacing and the applied voltage minimizes such effects.

The fiber mats from each of the four L-lysine concentrations were heated at 140°C for 1 h to drive the formation of cross-links. The nonwoven mats were found to contract slightly upon heat treatment, and to expand/contract again upon emersion in water and drying. Scanning electron micrographs of the heated poly(acrylic acid) electrospun fibers showed that heating of the fibers did not have any effect on their appearance. The temperature of 140°C was selected because it provides an adequate reaction rate but is well below 150°C where significant degradation of poly(acrylic acid) occurs.

Analysis of the scanning Electron Micrographs, using at least 50 fibers from each of the electrospun membranes described above, yielded the average diameter and standard deviation for each. The measurements demonstrated that nanoscale fiber diameters were obtained, with an average diameter of around 510(±60) nm and that no significant change in fiber diameter occurred on cross-linking. The inclusion of small amounts of lysine had little or no effect on the mean diameter.

The eight electrospun membranes were immersed in water overnight. Those that contained the lysine cross-linker and had been heated remained completely intact. Those that were not heated or did not contain the lysine dissolved; confirming the cross-linking action and heat activation of the L-lysine.

To measure the formation of any covalent crosslinks, FTIR spectroscopy was performed on all the samples before and after heating. Typical spectra of each are presented in Figures 3–6. The region between 1800 and 800  $\text{cm}^{-1}$  is presented in each case as this is where the most relevant peaks occur. In Figure 3 the typical spectra of electrospun poly(acrylic acid) before (solid line) and after heating is presented (140°C 2 h, broken line). There is very little difference between the two spectra. The combination of the strong carbonyl absorbance<sup>12–14</sup> (symmetric stretch) at 1705  $\text{cm}^{-1}$ , the C—O stretching mode at 1450 and the O—H in-plane bending at around 1248  $\text{cm}^{-1}$  are attributed to the carboxylic acid groups on the poly(acrylic acid).

When L-lysine was incorporated in the electrospinning solution, broad peaks for the free amino acid near 1620  $\text{cm}^{-1}$  (attributed

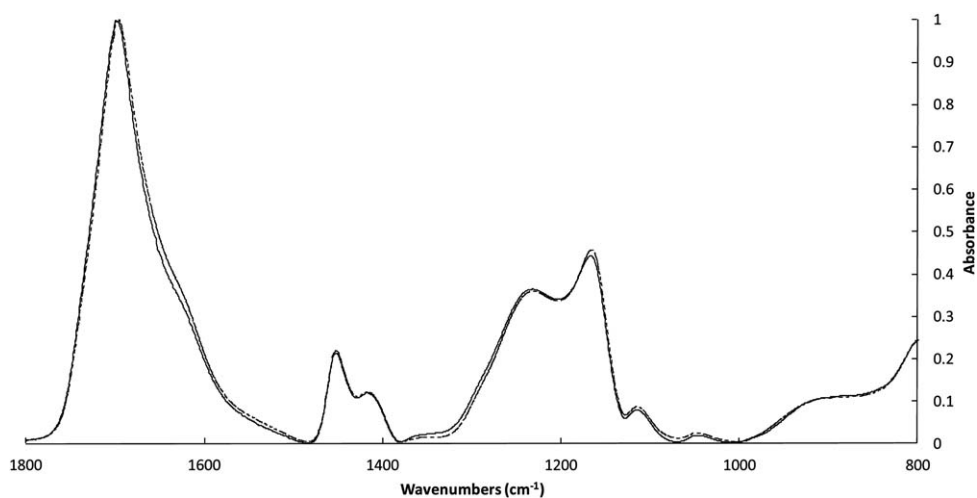


Figure 3. The FTIR spectrum of electrospun 8% poly(acrylic acid) before heating (dashed line) and after heating (solid line).

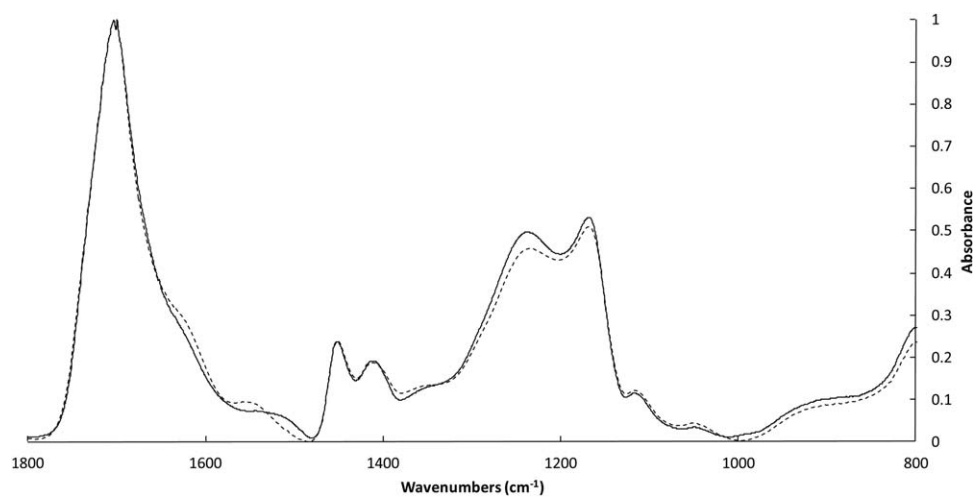
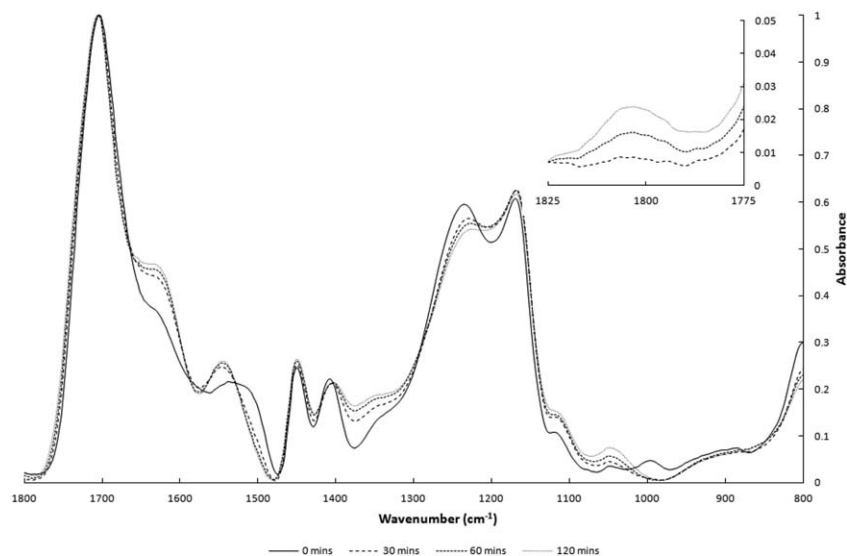


Figure 4. The FTIR spectrum of electrospun 8% poly(acrylic acid)/0.4% lysine before heating (dashed line) and after heating (solid line).



Figure 5. The FTIR spectrum of electrospun 8% poly(acrylic acid)/0.8% lysine before heating (dashed line) and after heating (solid line).





**Figure 6.** The FTIR spectrum of electrospun 8% poly(acrylic acid)/1.6% lysine heated for 0, 30, 60, and 120 min. Inset shows the  $1803\text{ cm}^{-1}$  peak for 30–120 min on an expanded scale.

to both an asymmetric amine deformation and a carbonyl symmetric stretch), and  $1515\text{ cm}^{-1}$  (amine symmetric stretch) were observed. The position of these two peaks is affected by the matrix in which they are dispersed,<sup>15</sup> shifting them to higher energy as compared with the solid pure lysine. The two mentioned peaks attributed to the lysine become more obvious as its concentration is increased in the spinning solution (comparing dashed curves in Figures 3–5).

When the fibers were heated to  $140^\circ\text{C}$  for 1 h, it was expected that water would be expelled and amide bonds formed. As the lysine peak near  $1620\text{ cm}^{-1}$  overlaps with the position of the Amide I band, only a change in shape of the peak at this position is observed. The lysine peak at  $1515\text{ cm}^{-1}$  (for the amine) changes significantly and is replaced by the Amide II band at

$1545\text{ cm}^{-1}$  as the amine moieties change into amides. Absorption peaks caused by the presence of amide bonds are expected at around  $1627$  and  $1534\text{ cm}^{-1}$  [as seen in poly(lysine)],<sup>16</sup> corresponding to the amide I and amide II bands.<sup>11</sup> As the amide peaks are superimposed upon a much larger carbonyl stretch at  $1705\text{ cm}^{-1}$  the precise peak shape and position are slightly skewed. The features attributed to the amide formation, absent in Figure 3, become obvious in Figure 4 (lowest lysine), and more obvious at a higher lysine content, as shown in the spectra of Figure 5.

To demonstrate the formation of these bonds as a function of heating time, the FTIR spectra of membranes electrospun from poly(acrylic acid) with 1.6% L-lysine that were heated for 0, 30, 60, and 120 min are presented in Figure 6. The amide peaks

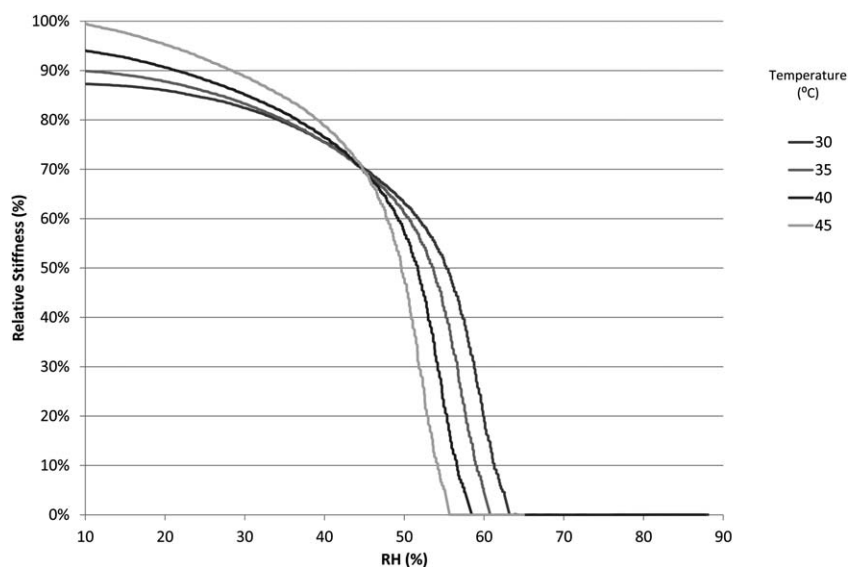


**Figure 7.** DMA plot of relative stiffness as a function of humidity at a range of temperatures. This sample had no cross-linking agent and so failed at  $45^\circ\text{C}$  and high humidity.

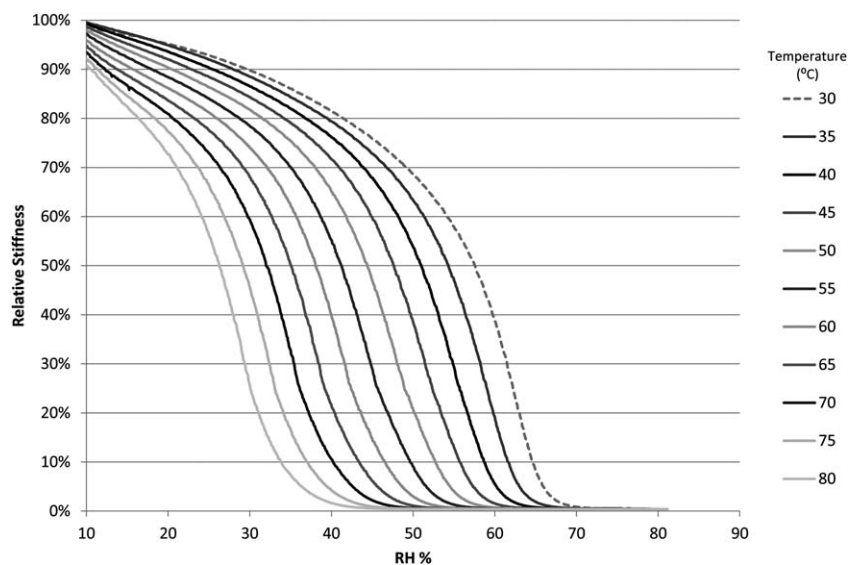


Figure 8. DMA heat and humidity sensitivity for the sample with 0.4% lysine.

seen to grow near  $1627\text{ cm}^{-1}$  and  $1534\text{ cm}^{-1}$  show that the majority of these bonds were formed in the first 30 min, with only small further increases after that time. As the carbonyl stretching peak at  $1705\text{ cm}^{-1}$  and the amide shoulder around  $1627\text{ cm}^{-1}$  have different extinction coefficients an absolute quantification of cross link density is not possible. The stability of all the fibers containing L-lysine suggest that only a small number of crosslinks are required to stabilize the electrospun fibers against dissolution in water. As two amide bonds must be formed between adjacent chains to form a crosslink, neither the consumption of L-lysine nor the number of amide bonds directly determines the number of crosslinks formed. However, an increase in the number of amide bonds would be expected correlate with an increase in crosslinking in this system.

Upon heating a small peak is also observed at around  $1803\text{ cm}^{-1}$  (see inset) and is attributed to the formation of acid anhydride groups as a consequence of reaction between adjacent carboxylic acid groups. The symmetric stretch is seen at  $1803\text{ cm}^{-1}$  while the asymmetric stretch near  $1740\text{ cm}^{-1}$  is hidden by the strong carbonyl peak at  $1705\text{ cm}^{-1}$ . Formation of acid anhydrides in this system was described elsewhere.<sup>12</sup> These groups are well known to be very sensitive to the presence of water vapor and so it was unsurprising that the peak seen in dry samples was found to disappear if they were held in humid conditions for a week or if immersed in water. Thus, these anhydride crosslinks between adjacent side chains on the poly(-acrylic acid) do not contribute to the long-term stability of the membranes.

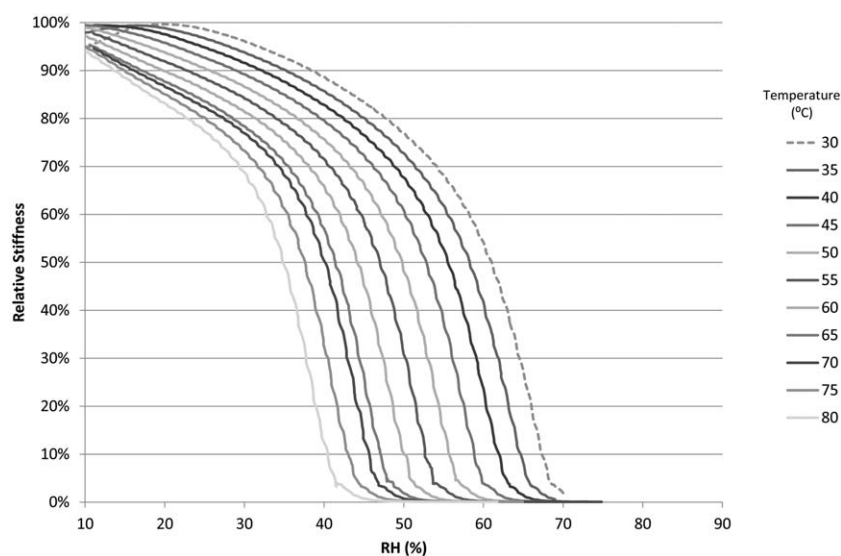


Figure 9. DMA heat and humidity sensitivity for the sample with 0.8% lysine.

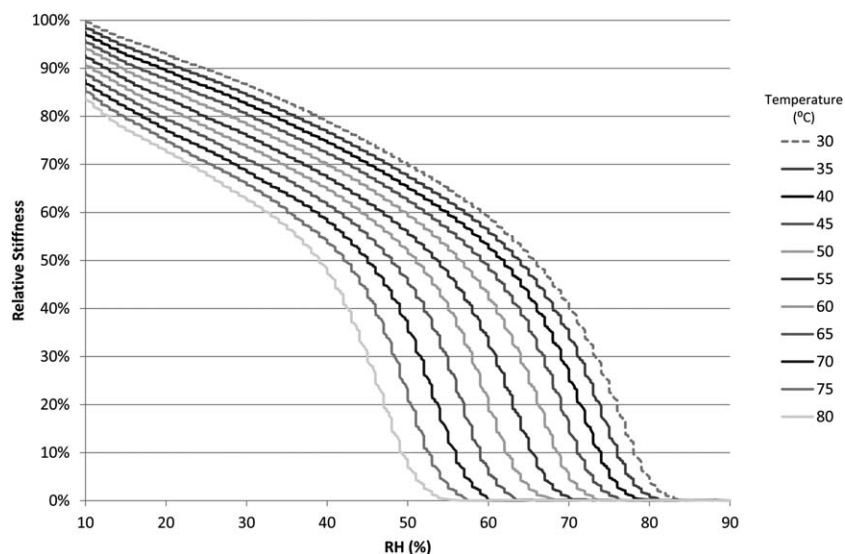


Figure 10. DMA heat and humidity sensitivity for the sample with 1.6% lysine.

### Dependence of Mechanical Properties on Humidity and Temperature

As the material is hygroscopic the mechanical properties are expected to depend strongly on the relative humidity as well as the temperature of the environment in which they are used.<sup>16</sup> To determine the dependence of this heat and moisture sensitivity on the degree of polymer cross-linking, Dynamic Mechanical Analysis (DMA) was undertaken using a device with a controlled humidity chamber. The device was programmed to run slowly through a series of relative humidity cycles from around 10% to 80% at a range of temperatures from 30 °C to 80 °C. After each cycle from ~10% RH to 80% and back to 10% RH, the temperature was incremented by 5 °C as was shown in Figure 1.

Figures 7–10 show the relative stiffness plotted against RH% for each temperature. There is a separate figure for each level of

cross-linker used and a separate curve for each temperature step. They all showed decreasing stiffness as the RH was increased from 10 to 80% and a glass transition was seen to occur at lower RH as the temperature is increased. The sample which had no cross-linking agent failed prematurely at only 45 °C and 55% RH (Figure 7).

At each temperature, the cross-linked samples in Figures 8–10 softened at higher RH with increasing cross-link density. As each RH scan is isothermal and the materials are likely to be used in isothermal conditions but with varying humidity, it is appropriate to describe their behavior with a glass transition relative humidity,  $RH_g$ , analogous to the more commonly used glass transition temperature,  $T_g$ . When the equilibrium moisture content is known for the material it may be appropriate to use the glass transition moisture content,  $MC_g$ . The glass transition

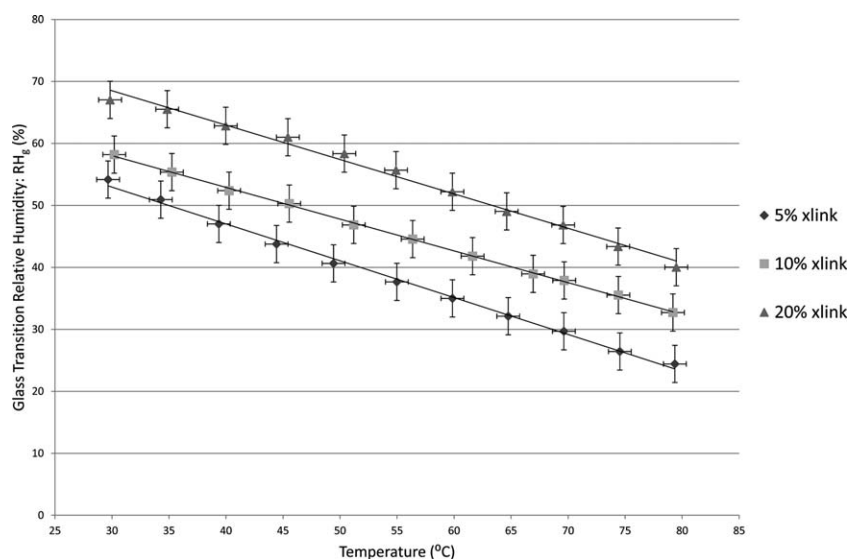
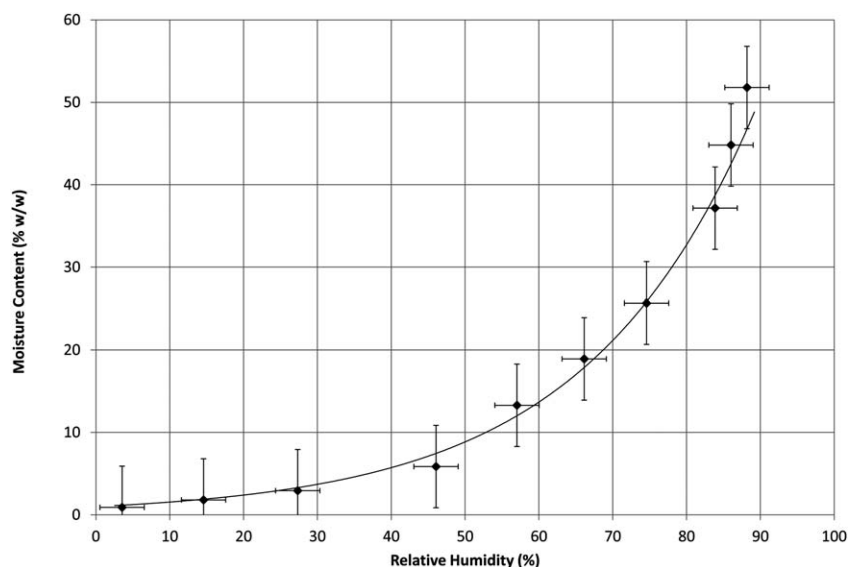


Figure 11. The glass transition relative humidity ( $RH_g$ ) as a function of temperature for the three levels of cross-linking.



**Figure 12.** Moisture absorption (%w/w) isotherm of the 20% cross-linked sample as a function of relative humidity at 40°C measured gravimetrically with the same rate of change in humidity as in the DMA measurements.

RH in this work was calculated in a similar way to that in which  $T_g$  would be calculated from a temperature scan, i.e., the onset point was found in the stiffness curve from the value of RH at the intersection of the extrapolated slopes just before and just after the glass transition.

All the samples show a steadily decreasing stiffness and reduction of  $RH_g$  as the temperature increases, as would be expected. To illustrate this further, Figure 11 is a graph of the  $RH_g$  value plotted against temperature. This clearly shows how the sensitivity to moisture increases with increasing temperature and how the effect of RH is reduced with increasing cross-link density. Figure 11 is essentially a plot of the RH at which the glass transition occurs for each (constant) temperature at which the RH scan was conducted. The glass transition occurs when the

polymer molecules are mobile enough to allow cooperative segmental motion which results in a change in polymer properties from glassy to rubbery. Chain mobility is increased by the presence of water molecules, which act as a plasticizer, as well as by increasing the temperature. Thus as the temp is increased less moisture is needed to reach the glass transition (Figures 11 and 13). Crosslinking reduces chain mobility so samples with increased lysine content need more moisture at the same temperature to achieve a given level of mobility (Figure 11). The increase in crosslinking is evidenced by the improved relative stiffness of the samples at higher relative humidity. Relative stiffness is compared because absolute stiffness is sensitive to fiber diameter, density, and sample thickness, in addition to moisture content, which makes the comparison more difficult.

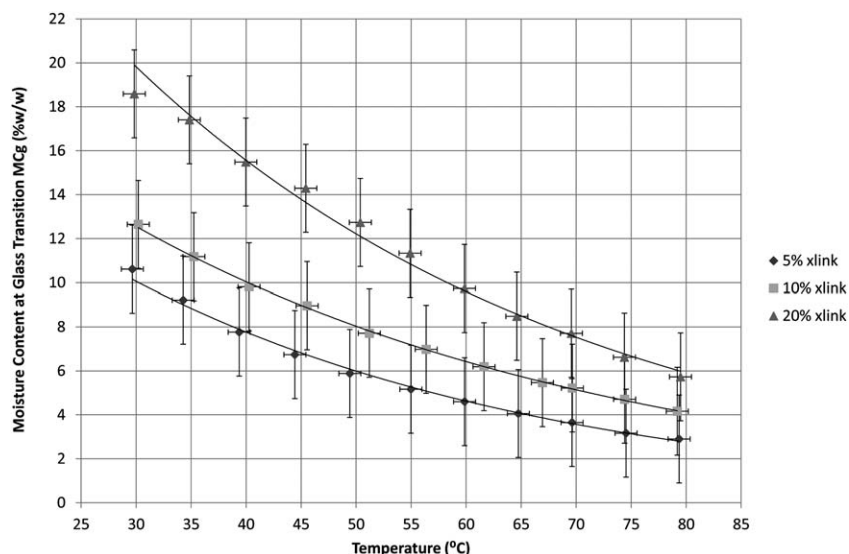


**Figure 13.** The glass transition moisture content ( $MC_g$ ) of the cross-linked electro-spun PAA membranes as a function of temperature.



The fineness of the electrospun fibers leads to high specific surface area and rapid equilibration with the moisture in the air so it is reasonable to assume that the slow ramp maintains moisture equilibrium between the fibers and the air. The moisture content of the membranes was measured gravimetrically at 40°C in a chamber with controlled temperature and humidity and with a similar rate of change of relative humidity as was used in the DMA measurements. The result for a 1.6% Lysine, 20% cross-linked membrane is shown in Figure 12. These data were used to plot the depression of  $MC_g$  as a function of temperature in Figure 13.

## CONCLUSIONS

Poly(acrylic acid) has been successfully electro-spun into nanoscale fibers and the effects of varying the concentration of the lysine cross-linking agent have been studied. Lysine was chosen to allow discrimination of cross-link peaks in FTIR from existing polymer bonds. The spectroscopic analysis showed qualitatively the dependence of cross-link density on the concentration of lysine in the spinning solution and the time evolution of the cross-link density when curing at 140°C.

The mechanical properties of the membranes were shown to be sensitive to temperature and humidity and the influence of cross-link concentration on these properties was quantified. Isothermal glass-transitions as a function of moisture content were measured using DMA over a range of temperatures, allowing the definition of glass-transition moisture content, which in some applications is more useful than a glass transition temperature that varies with moisture content. The extreme loss of stiffness with high moisture content suggests that PAA membranes would need mechanical support if used in circumstances where high RH may be experienced. It was shown that the sensitivity of the membranes to moisture and heat could be reduced by increasing the number of cross-links. Further increases in cross-linking agent may lead to greater increases in stability but would also influence absorbency and swelling behavior.

## ACKNOWLEDGMENTS

The authors would like to thank Debra Hamilton and Lucy Vuckovic for their experimental assistance, and Colin Veitch for obtaining the electron microscope images.

## REFERENCES

1. Doshi, J.; Reneker, D. H. *J. Electrostat.* **1995**, *35*, 151.
2. Greiner, A.; Wendorff, J. H. *Nanotechnology* **2007**, *46*, 5670.
3. Li, D.; Xia, Y. *Adv. Mater.* **2004**, *16*, 1151.
4. Reneker, D. H.; Yarin, A. L. *Polymer* **2008**, *48*, 2387.
5. Aussawasathien, D.; Teerawattananon, C.; Vongachariya, A. *J. Membr. Sci.* **2008**, *315*, 11.
6. Truong, Y. B.; Kyrtziz, I. L.; Shen, W. *J. Mater. Sci.* **2009**, *44*, 1101.
7. Xiang, C. H.; Frey, M. W.; Taylor, A. G.; Rebovich, M. E. *J. Appl. Polym. Sci.* **2007**, *106*, 2363.
8. Jianqi, F.; Lixia, G. *Eur. Polym. J.* **2002**, *38*, 1653.
9. Gestos, A.; Whitten, P. G.; Spinks, G. M.; Wallace, G. G. *Soft Matter* **2010**, *6*, 1045.
10. Chen, Z.; Cao, L.; Wang, L.; Zhu, H.; Jiang, H. *J. Appl. Polym. Sci.* **2013**, *127*, 4225. doi: 10.1002/app.38000.
11. Liu, Y. R.; Geever, L. M.; Kennedy, J. E.; Higginbotham, C. L.; Cahill, P. A.; McGuinness, G. B. *J. Mech. Behav. Biomed.* **2010**, *3*, 203.
12. Coates, J. In *Encyclopedia of Analytical Chemistry*, Meyers, R. A., Ed.; Wiley: Chichester, **2000**, p 10815.
13. Dong, J.; Ozaki, Y.; Nakashima, K. *Macromolecules*, **1997**, *30*, 1111.
14. Pretsch, E.; Bühlmann, P.; Badertscher, M. *Structure Determination of Organic Compounds*, Springer: Berlin, **2000**.
15. Mutha, S. C.; Ludemann, W. B. *J. Pharma. Sci.* **1976**, *65*, 1400.
16. Rozenberg, M.; Shoham, G. *Biophys. Chem.* **2007**, *125*, 166.
17. Naficy, S.; Kawakami, S.; Sadegholvaad, S.; Wakisaka, M.; Spinks, G. M. *J. Appl. Polym. Sci.* **2013**, *130*, 2504.